ORIGINAL ARTICLE

Lingzhi and San-Miao-San with hyaluronic acid gel mitigate cartilage degeneration in anterior cruciate ligament transection induced osteoarthritis

Man Chu [a], Ping Wu [b], Ming Hong [c,d], Huasong Zeng [b], Chun Kwok Wong [e], Yu Feng [f,*], Zhe Cai [b,e,g,h,**], William Weijia Lu [i,j,***]

[a] Faulty of Medical Technology, Shaanxi University of Chinese Medicine, Xianyang, China
[b] Department of Allergy, Immunology and Rheumatology, Guangzhou Women and Children's Medical Center, Guangzhou, Guangdong, China
[c] Science and Technology Innovation Center, Guangzhou University of Chinese Medicine, Guangzhou, China
[d] Institute of Clinical Pharmacology, Guangzhou University of Chinese Medicine, Guangzhou, China
[e] Department of Chemical Pathology, The Chinese University of Hong Kong, Prince of Wales Hospital, Hong Kong, China
[f] Department of Traumatology, General Hospital of Ningxia Medical University, Yinchuan, Ningxia Hui Autonomous Region, China
[g] The Joint Center for Infection and Immunity, Guangzhou Institute of Pediatrics, Guangzhou Women and Children's Medical Center, Guangzhou, China
[h] The Joint Center for Infection and Immunity, Institute Pasteur of Shanghai, Chinese Academy of Science, Shanghai, China
[i] Department of Orthopaedics and Traumatology, Li Ka Shing Faculty of Medicine, The University of Hong Kong, Hong Kong
[j] Shenzhen Institutes of Advanced Technology, Chinese Academy of Science, Shenzhen, China

SUMMARY

Objective: To investigate the mitigate efficacy of Chinese medicine Lingzhi (LZ) and San-Miao-San (SMS) combined with hyaluronic acid (HA)-gel in attenuating cartilage degeneration in traumatic osteoarthritis (OA).

Methods: The standardized surgery of anterior cruciate ligament transection (ACLT) was made from the medial compartment of right hind limbs of 8-week-old female SD rats and resulted in a traumatic OA. Rats (n = 5/group) were treated once intra-articular injection of 50 μl HA-gel, 50 μl HA-gel+50 μg LZ-SMS, 50 μl of saline+50 μg LZ-SMS and null (ACLT group) respectively, except sham group. Limbs were harvested for μCT scan and histopathological staining 3-month post-treatment. Inflammatory cytokines from plasma and synovial fluid were detected using Immunology Multiplex Assay kit. The putative targets of active compounds in LZ-SMS and known therapeutic targets for OA were combined to construct protein–protein interaction network. Gene Ontology and Kyoto Encyclopedia of Genes and Genomes (KEGG) enrichment analysis was adopted to predict the potential targets and signaling pathway of LZ-SMS in OA through the tool of DAVID Bioinformatics.

Results: In vivo, HA-gel + LZ-SMS treatment resulted in a higher volume ratio of hyaline cartilage (HC)/calcified cartilage (CC) and HC/Sum (total volume of cartilage), compared to ACLT and HA-gel groups. In addition, histological results showed the elevated cartilage matrix, chondrogenic and osteoblastic signals in HA-gel + LZ-SMS treatment. Treatment also significantly altered subchondral bone (SCB) structure including an increase in BV/TV, Tb.Th, BMD, Conn.Dn, Tb.N, and DA, as well as a significant decrease in Tb.Sp and Po(tot), which implied a protective effect on maintaining the stabilization of tibial SCB microstructure. Furthermore, there was also a

down-regulated inflammatory cytokines and upregulated anti-inflammatory cytokine IL-10 in HA+LZ-SMS group. Finally, 64 shared targets from 37 active compounds in LZ-SMS related to the core genes for the development of OA. LZ-SMS has a putative role in regulating inflammatory circumstance through influencing the MAPK signaling pathway.

Conclusion: Our study elucidated a protective effect of HA-gel + LZ-SMS in mitigating cartilage degradation and putative interaction with targets and signaling pathway for the development of traumatic OA.

The translational potential of this article: Our results provide a biological rationale for the use of LZ-SMS as a potential candidate for OA treatment.

Introduction

Osteoarthritis (OA) is one of the most common types of arthritis characterized by inflammation, abnormal remodeling of subchondral bone (SCB), chronic degeneration of articular cartilage (AC) and osteophyte formation [1]. Significant superficial cartilage (SC) damage, hyaline cartilage (HC) thinning and accelerated SCB resorption are demonstrated in an anterior cruciate ligament transection (ACLT) induced OA rat model, which mimicked human traumatic OA, to assess tissue alterations including type II collagen and aggrecan (Acan) degradation, and chondrocyte loss, which are eventually leading to a progressive OA [2,3].

The interaction between SCB and AC in the pathogenesis of traumatic OA has been drawn attention [4–7], and it is postulated that the pathological changes in the structure and function of SCB play a pivotal role in the OA pathogenesis [8–11], and then influence the integrity and function of AC. The changes in organization and composition of SCB lead to abnormal remodeling in response to the unstable stress states in the progression of OA, and affect the overlying AC adversely [11]. For instance, the abnormal SCB turnover at the osteochondral conjunction may impede molecular communication between bone and cartilage during the development of OA, and may lead to an invasion of calcified cartilage (CC) into middle zone of cartilage (MZ), then finally results in HC thinning [12,13]. The invaded CC is correlated with the chondrocyte hypertrophy, which contributes to the cartilage ossification [14,15]. Therefore, the integrity of AC has been proposed to depend on the biomechanical properties of the underlying SCB [7].

Mechanical stresses caused joint instability is considered to have induced the alterations of biochemical factors which lead to focal degradation of AC in the affected joints [9]. Chondrocytes can sensitively respond to the variation of microenvironment in the joints and regulate the dynamic equilibrium between the synthesis and degradation of cartilage extracellular matrix (ECM), which plays a key role in maintaining the function of cartilage [16]. Due to the erosion of ECM at SC and HC area, this results in a gradual disruption of AC intactness [17], and finally exacerbates the progression of OA. Therefore, the functional changes in chondrocytes play a pivotal role in the AC degeneration, and promoting the proliferation of chondrocytes could be one of important strategies for the maintenance of cartilage structure [18].

Recently, most of the classic conservative therapies intended to mitigate pain, which is the most prominent symptoms of OA, rather than modifying this disease. Actually, these therapies in alleviating the progression of OA have limited efficacy, and eventually have led the advanced patients to receive surgical treatments [19]. Thus, there is an unmet requirement for exploring a new treatment to slow down the traumatic OA progression. In clinic, one of the new minimally-invasive therapies to mitigate the joint pain is the intra-articular injection of hyaluronic acid (HA) hydrogels [20]. In addition, hyaluron secreted by the chondrocytes could enhance joint lubrication and helped to prolong the efficacy of growth factors by binding and slowly releasing them as HA-gel degrades [21]. However, clinical studies report that this treatment only provides transient remission of OA symptoms, and the therapeutic efficacy remains ambiguous [22]. Currently, most of the studies engage in enhancing the efficacy of HA hydrogels, such as through combining HA-gel to the traditional Chinese medicine (TCM) for further synergistic therapy of OA [23].

According to the belief in Chinese medicine, LZ-SMS is one of the most widely distributed naturally occurring quaternary aporphine alkaloids, and one of key compounds of Huang Bo (Cortex phellodendri), an effective herb in the TCM formula San-Miao-San, which was used to treat arthritis over hundreds of years [24–26]. Some previous studies demonstrated that LZ-SMS exerted significant anti-inflammatory effects, and as the main active ingredient potentially promoted synthesis of proteoglycans in chondrocytes, then reversed the progression of rheumatoid arthritis [27,28]. However, the underlying beneficial effect of LZ-SMS on traumatic OA has not been completely investigated. We thereby would study the new role of LZ-SMS using the ACLT induced traumatic OA model to illustrate the latent therapeutic effect on attenuating the degeneration of AC by activating the chondrogenic signaling pathway and bioinformatics analysis of potential drug targets.

Materials and methods

Animal model and treatment

The Ethics Committee On The Use Of Live Animals In Teaching & Research (CULATR) of The University of Hong Kong (HKU) approved all of the protocols (CULATR Ref. No.: 4004-16) and procedures in this study. The standardized surgery of ACLT was made on the right hind limb of 8-week-old female SD rat (250–260 g/rat) to induce the model of post-traumatic knee OA following a well-established protocol as previously described [29]. After one month of ACLT surgery, 20 operated rats were randomly divided into 4 groups (HA, HA+LZ-SMS, LZ-SMS and ACLT group, n = 5/group), and received once two weeks in a single dose intra-articular injection with 50 μl of HyStem-HP® HA gel (ESI BIO Products of Ascendance Biotechnology, Alameda, CA, USA) (HA group), 50 μl of HA gel with 50 μg of purified LZ-SMS (PuraPharm International, Hong Kong, China) (HA+LZ-SMS group), 50 μl of saline with 50 μg of purified LZ-SMS (LZ-SMS group), or no treatment (ACLT group) for 3 consecutive months. All of these injection reagents were sterilized by 0.22 μm syringe filter (Merck Millipore, Billerica, MA, USA). The Sham group (n = 5) was received the same operation but without ACLT operation. Then the rats were sacrificed at about 6 month-old to harvest the hind knee joints for micro-CT scans and histopathological evaluation. The blood and synovial fluid were obtained for cytokines assay.

Micro-CT analysis

Collected knee joints were fixed in 10% neutral buffered formalin and scanned using a high resolution micro-CT system (model 1076, SkyScan, Kontich, Belgium). The 329 projections for each sample were produced with the following settings: Isotropic voxel 17.3 μm, voltage 100 kV, current 100 mA, and exposure time 320 ms, frame averaging 2, beam filtration filter 1.0 mm aluminum. After scanning, the data sets were then reoriented using DataViewer (version 1.4.4.0, SkyScan) to analyze in the sagittal plane. Binarization of the images with a global thresholding of gray levels (56–106), the calculation of morphological parameters was carried out with the CTAn software (version 1.13.2.1, SkyScan). The trabecular bone volume fraction (BV/TV, %), connectivity density (Conn.Dn, $1/mm^3$), trabecular thickness (Tb.Th, mm), trabecular number (Tb.N), trabecular bone pattern factor (Tb.Pf, 1/mm), trabecular separation (Tb.Sp, mm), degree of anisotropy (DA) and trabecular bone total

porosity (Po(tot), %) were measured [30]. Bone mineral density (BMD) (g/cm^3) was calibrated by using the attenuation coefficient of two hydroxyapatite phantoms with defined mineral density of 0.25 and 0.75 g/cm^3. Additionally, for analysis of subchondral trabecular bone degeneration, a cuboid of load bearing region in the middle area of medial tibial close to SCB plate was selected as Region of Interest (ROI, blue rectangle area, Fig. 1A and B) in size of $0.554 \times 0.346 \times 0.277 \, mm^3$ to do the three-dimensional (3D) reconstruction (Fig. 1B) by the CTvol software (version 1.13.2.1, SkyScan).

Toluidine Blue, Tartrazine and Fast Green staining

The knee joints from rats in each group were harvested to evaluate the pathological degeneration of articular cartilage (Figs. 1 and 2). All tissues were fixed in 4% paraformaldehyde and were decalcified in 0.5 M EDTA-Na_2 (pH 7.5) at room temperature. They were dehydrated in the gradient concentrations of ethanol, then cleared in xylene, and lastly embedded in paraffin. The embedded samples were sectioned into 5 μm using Leica RM2135 microtome (Leica Microsystems; Wetzlar, Germany). The slides of central region of the medial tibial plateau were sequentially stained with a TTF multichromatic histological staining: Toluidine Blue (0.04% w/v in 0.1M sodium acetate), Tartrazine solution (0.025% w/v in 2.5% acetic acid) and 0.1% Fast Green solution [3]. Meanwhile, the volume ratio of HC/CC, the relative volume of HC, CC and SC, and the volume ratio of HC/whole cartilage (Sum) were quantified by Image Pro-Plus software (version 6.0.0.260, Media Cybernetics, Rockville, MD). At least three paraffin sections of each sample from each group (n = 5) were measured.

Immunohistochemistry analysis

Sections were deparaffinized in xylene and rehydrated in gradient alcohol, and underwent heat-induced antigen retrieval using Target Retrieval Solution (Dako, Carpinteria, CA). The slides were then quenched in Dako REAL™ Peroxidase-Blocking Solution (Dako) and blocked in 5% goat serum (Invitrogen, USA) followed by incubation with primary antibodies anti-RANKL (Acan, 1:50, service bio, Inc., Wuhan, China), anti-BMP2 (1:100, service bio, Inc., Wuhan, China) and anti-transforming growth factor beta (TGF-β)-1 (1:100, service bio, Inc.,

Wuhan, China) at 4°C overnight. Subsequently, the sections were incubated with horseradish peroxidase conjugated IgG H&L secondary antibody (1:1000, Abcam) for 1 h in room temperature and visualized using the liquid 3, 30-diaminobenzidine (DAB)+ substrate-chromogen system (Dako).

Cytokines and chemokines assay

Rat cytokine Milliplex MAP kit was purchased from Merck Millipore (Billerica, MA, USA). This kit included the antibody-immobilized magnetic beads, detection antibody, and streptavidin-phycoerythrin. It allowed measuring multiple cytokines or chemokines in one reaction by using the Bio-plex 200 System (Bio-Rad Laboratories, Inc. CA, USA). Concentrations of IL-6, IFN-γ, TNF-α, IL-12p70, IL-17A and IL-10 in synovial fluids and plasma were quantitated using rat cytokine Milliplex MAP kit.

Identification of active compounds and related targets in LZ-SMS

To determine the chemical ingredients of the four herbs contained in LZ-SMS, we performed a search by Traditional Chinese Medicine Systems Pharmacology Database (TCMSP, Version: 2.3, http://lsp.nwu.edu.cn/tcmsp.php). The absorption, distribution, metabolism, and excretion (OAME) system used in this study includes predict oral bioavailability (OB) and drug-likeness (DL), and compounds were retained only if OB > 30 and DL > 0.18 to satisfy criteria suggested by the TCMSP database [31]. The integrative efficacy of the ingredients in LZ-SMS was determined by analyzing the ingredients and targets interactions obtained from TCMSP Database.

Prediction of the therapeutic targets acting on OA

We collected OA targets from two sources. One is the GeneCards database [32] (https://www.genecards.org/, version 4.12), which provides comprehensive information on all annotated and predicted human genes and the keywords. The other resource was the Online Mendelian Inheritance in Man (OMIM) database (http://www.omim.org/, updated on Nov 21, 2019) [33]. The OMIM database catalogued all known diseases with a genetic component and linked them to the relevant genes in
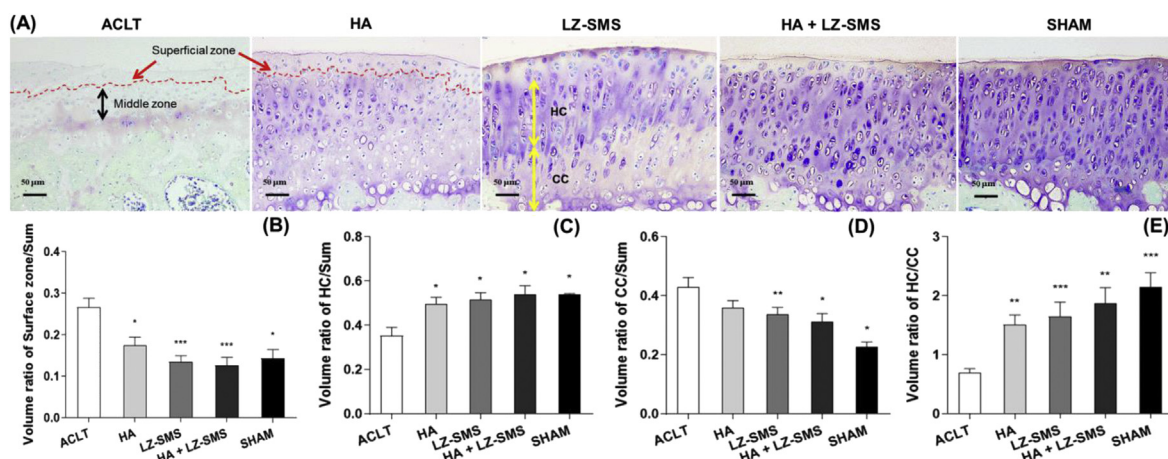

Figure 1. Histological images and quantitative analysis of rat tibial plateau in different groups. (A) The representative images of toluidine blue, tartrazine and fast green stained the tibial medial articular cartilage in different treatment groups. Light color stained superficial zone of articular cartilage (SZ) pointed by the red arrow and by the red dash line separated area were shown in ACLT and HA groups. The black and yellow bidirectional arrows pointed the middle zone of articular cartilage (MZ) and thickness of hyaline cartilage (HC) and calcified cartilage (CC) in ACLT and LZ-SMS groups, respectively. Scale bar, 50 μm. (B–E) The Bar charts are shown the quantitative analyzed volume ratios at different zone of cartilage in each group tibial plateau. They are volume ratios of SZ/Sum (total volume of cartilage), HC/Sum, CC/Sum and HC/CC. Differences among treatments are compared by one-way ANOVA (n = 5/group, *p < 0.05, **p < 0.01, ***p < 0.0001, ACLT vs. other groups). Wilcoxon test is used to assess the differences between two different treatments (n = 5/group, p > 0.05, HA+LZ-SMS vs. other groups). (For interpretation of the references to colour in this figure legend, the reader is referred to the Web version of this article.)
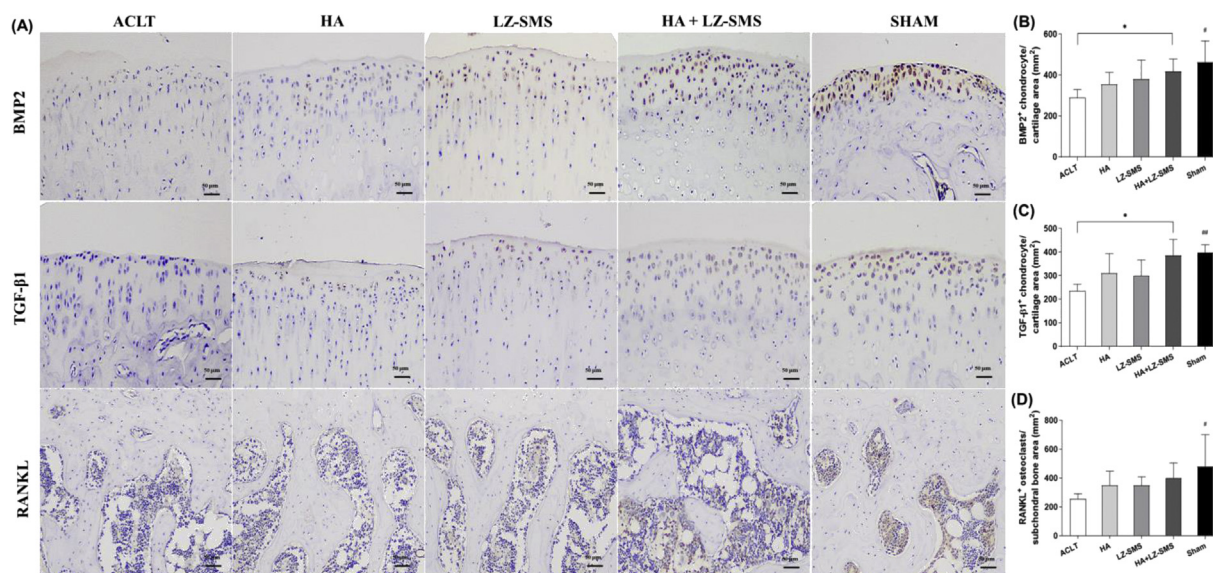
Figure 2. Immunohistochemistry images and quantitative analysis of chondrogenic and osteoblastic signals in different groups. (A) The representative images of BMP2+ and TGF-β1+ chondrogenic cells and RANKL+ osteoblasts are shown at articular cartilage and SCB plate area in different groups, respectively. Scale bar, 50 μm. The Bar charts are shown the quantitative analysis of the number of (B) BMP2+ and (C) TGF-β1+ cells per cartilage area (mm^2), and (D) RANKL+osteoblasts per SCB plate area (mm^2) in each group, respectively. Differences among treatments are compared by one-way ANOVA (n = 5/group, #p < 0.05, ##p < 0.01, ACLT vs. other groups). Wilcoxon test is used to assess the differences between two different treatments (n = 5/group,*p < 0.05, HA+LZ-SMS vs. other groups).

the human genome and provided references for further research and tools for genomic analysis of a catalogued gene [33].

Network construction and analysis

The overlapping targets between LZ-SMS and OA were selected. Then the interactions between proteins of the putative targets of active compounds in LZ-SMS, and known therapeutic targets for OA were combined to construct putative LZ-SMS target-known therapeutic targets of OA network. It can be applied to illustrate the relationships between putative targets contained in LZ-SMS and known therapeutic targets of OA. The graphical interactions in this network was visualized using Cytoscape software [34] (version 3.6.0, Boston, MA, USA).

Protein–protein interaction data

The data of protein–protein interaction (PPI) come from STRING (http://stringdb.org/, version 10) with the species limited to "*Homo sapiens*" and a confidence score >0.7. STRING is a database of known and forecasted protein–protein interactions [35]. Each node represents a protein and each edge represents an interaction. The more these edges are, the more important the node is in the network.

Gene ontology and KEGG enrichment analysis for targets

The gene ontology (GO) which involves biological process (BP), molecular function (MF), and cellular component (CC) was analyzed to further validate whether the potential targets are indeed related to OA. Kyoto Encyclopedia of Genes and Genomes (KEGG) enrichment analysis was adopted to predict the potential signaling pathway of LZ-SMS in OA. The GO and KEGG enrichment analysis were performed using the functional annotation tool of DAVID Bioinformatics Resources 6.7 (https://david-d.ncifcrf.gov/) [36]. After using Benjamini–Hochberg method to control the false discovery rate (FDR) for multiple hypothesis tests, the adjusted p value < 0.05 was used as the significance cutoff in our study.

Statistical analysis

All data were presented as the means ± SD. Since the sample size was small (n = 5/group in 5 group, 25 in total), Wilcoxon test was performed for comparison between two groups. The comparison of normally distributed variables in different groups was made with one-way analyses of variance (ANOVAs), followed by post hoc Bonferroni's test for comparing the differences and calculating a p value for each pair of comparison. All hypotheses were 2-tailed, and p values < 0.05 were considered significant. Analyses were performed using GraphPad Prism, Version 8 (GraphPad software, San Diego, CA, USA).

Results

LZ-SMS attenuated cartilage degeneration in ACLT induced OA rat

In ACLT group, a fluctuation with matrix loss and decreased proteoglycan contents were visualized in the superficial zone of articular cartilage (SZ, red arrow pointed area), and even further extended to middle zone (Fig. 1A). The distribution of matrix was heterogeneous with a severe loss of proteoglycan contents in the interterritorial matrix. In addition, we found obviously thicker SZ (red arrow pointed red dash line) in the ACLT and HA group (Fig. 1A and B, *p < 0.05, ***p < 0.0001). Furthermore, when compared to ACLT groups, the higher volume ratio of HC/Sum and lower volume ratio of CC/Sum represented a thicker HC in LZ-SMS, HA+LZ-SMS and Sham groups (*p < 0.05, **p < 0.01, Fig. 1C and D). Finally, the volume ratio of HC/CC was lower in ACLT groups than HA, LZ-SMS, HA+LZ-SMS and Sham groups (**p < 0.01, ***p < 0.0001), respectively (Fig. 1E). The above results may imply that to maintain the volume of HC was conducive for alleviating OA progression. The decreased volume ratio of HC/CC might be a biomarker for the degeneration of articular cartilage in ACLT induced OA. Therefore, the local administration of HA gel + LZ-SMS in knee joint could be a potential treatment for alleviating the decreased volume ratio of HC/CC and even impeded cartilage degeneration.

Enhancement of chondrogenic and osteoblastic signals promoted by HA gel + LZ-SMS

In the light of the protective effect on cartilage matrix, the quantitative analysis of chondrogenic signaling pathway revealed a significantly higher number of BMP2+ and TGF-β1+ chondrogenic cells at the MZ in HA gel + LZ-SMS treated rats (*p < 0.05, Fig. 2A–C), and lower number of RANKL+ osteoblasts at the trabecular SCB in the Sham group (#p < 0.05, Fig. 2D). All the results suggested the elevation of chondrogenic and osteoblastic signals reflected an enhanced chondrogenesis due to the HA gel + LZ-SMS treatment.

Anti-inflammatory effect of LZ-SMS

In vitro study, from the results of downregulated pro-inflammatory cytokines including IL-17A, IL-12p70, TNF-α, INF-γ and IL-6, as well as upregulated anti-inflammatory cytokine IL-10 in plasmid and synovial fluid (Fig. 3A and B), we firmly convinced that the LZ-SMS could perform a potential anti-inflammatory efficacy.

LZ-SMS prevented subchondral bone from un-stabilization in the ACLT induced OA

At 4-month post-surgery, obvious sclerosis of the load bearing area of medial tibial plateau (red arrow points in Fig. 4A) and trabecular bone cysts (green arrow pointed area in Fig. 4A) from ACLT rats rather than HA gel + LZ-SMS treated rats were shown in 3-view and 3D reconstruction images (Fig. 4A and B). Consistent with these appearances, the parameters of trabecular SCB microstructures in HA+LZ-SMS group had a significant increase (Fig. 4C), such as BV/TV (#p < 0.05) and Tb.Th (#p < 0.05), BMD (###p < 0.0001), Conn.Dn (###p < 0.0001), Tb.N (###p < 0.0001), DA (#p < 0.05), and a significant decrease like Tb.Sp (#p < 0.05) and Po(tot) (###p < 0.0001), which implied a protective effect of HA gel + LZ-SMS on maintaining the stabilization of trabecular SCB microstructure in ACLT induced OA. Therefore, these results suggested HA gel + LZ-SMS might involve in the resistance of SCB damage in

traumatic OA model.

Identification of active compounds and related targets in LZ-SMS

From the TCMSP, a total of 607 compounds were retrieved including 242 in *Ganoderma lucidum*, 140 in huangbo, 49 in cangzhu and 176 in niuxi. High OB is often a key indicator of bioactive molecules, and DL is a qualitative concept used in drug design for estimating the druggability of a substance. For active compound screening, OAME criteria OB > 30% and DL > 0.18 was adopted in the present study. As a matter of fact, 61 (25.2%) compounds in *G. lucidum*, 37 (26.4%) compounds in huangbo, 9 (18.4%) compounds in cangzhu and 20 (11.4%) compounds in niuxi satisfied the criteria of OB > 30% and DL > 0.18. Among the 607 compounds, a total of 127 satisfied all the aforementioned conditions and 117 compounds were finally obtained after excluding the duplicates (Supplementary Table S1). In total, 50 of the 117 compounds in LZ-SMS were associated with 108 target proteins from TCMSP.

The known therapeutic targets acting on OA

In total, 2 known therapeutic targets for the OA treatment were identified based on OMIM database. And 2496 known therapeutic targets for the treatment of OA were acquired based on GeneCards database. After combining these therapeutic targets and eliminating the redundancy, a total of 2497 known therapeutic targets in the treatment of OA were collected in this study.

Network analysis

The total of 64 intersected targets between LZ-SMS and OA were obtained and shown by Venn diagram (Fig. 5A, Supplementary Table 2), and these targets derived from 37 active compounds in LZ-SMS. Then the LZ-SMS active compound-target-OA disease network was visualized and shown as Fig. 5B. According to the network analysis, the key compounds involved in the treatment of OA are quercetin, wogonin, palmatine, inophyllum E, kaempferol, fumarine, baicalein and beta-sitosterol.
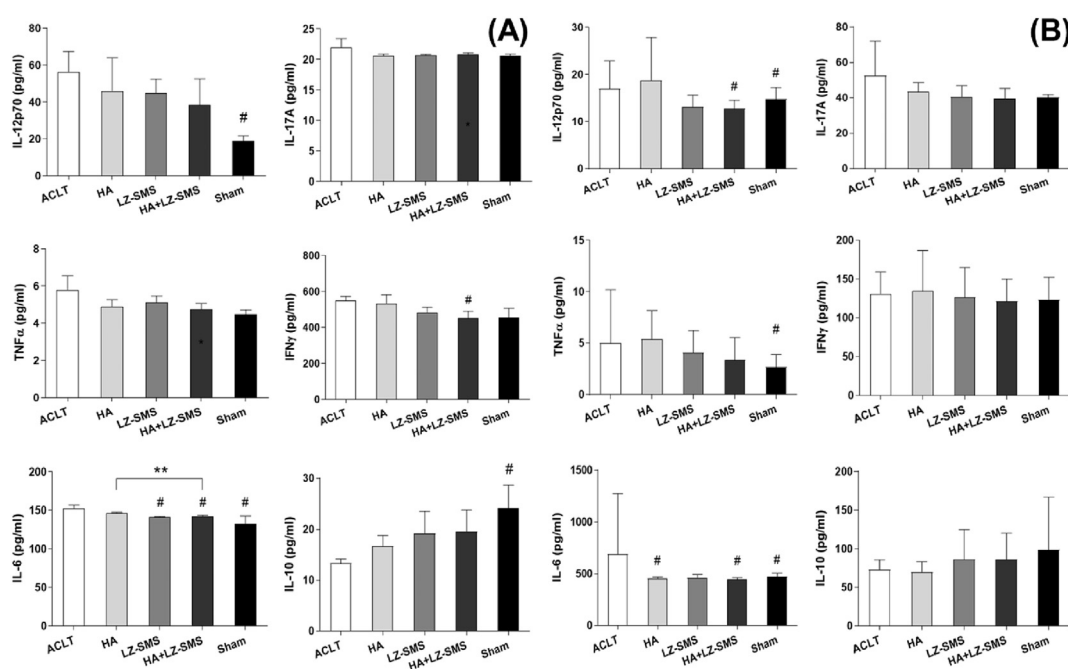

Figure 3. Anti-inflammatory LZ-SMS suppress pro-inflammatory cytokines in plasma and synovial fluid. The Bar charts are shown the levels of (A) plasma and (B) synovial fluid cytokines including IL-12p70, IL-17A, TNF-α, INF-γ, IL-6 and IL-10 from different treated groups. Differences among treatments are compared by one-way ANOVA (n = 5/group, #p < 0.05, ##p < 0.01, ACLT vs. other groups). Wilcoxon test is used to assess the differences between two different treatments (n = 5/group,*p < 0.05, HA+LZ-SMS vs. other groups).
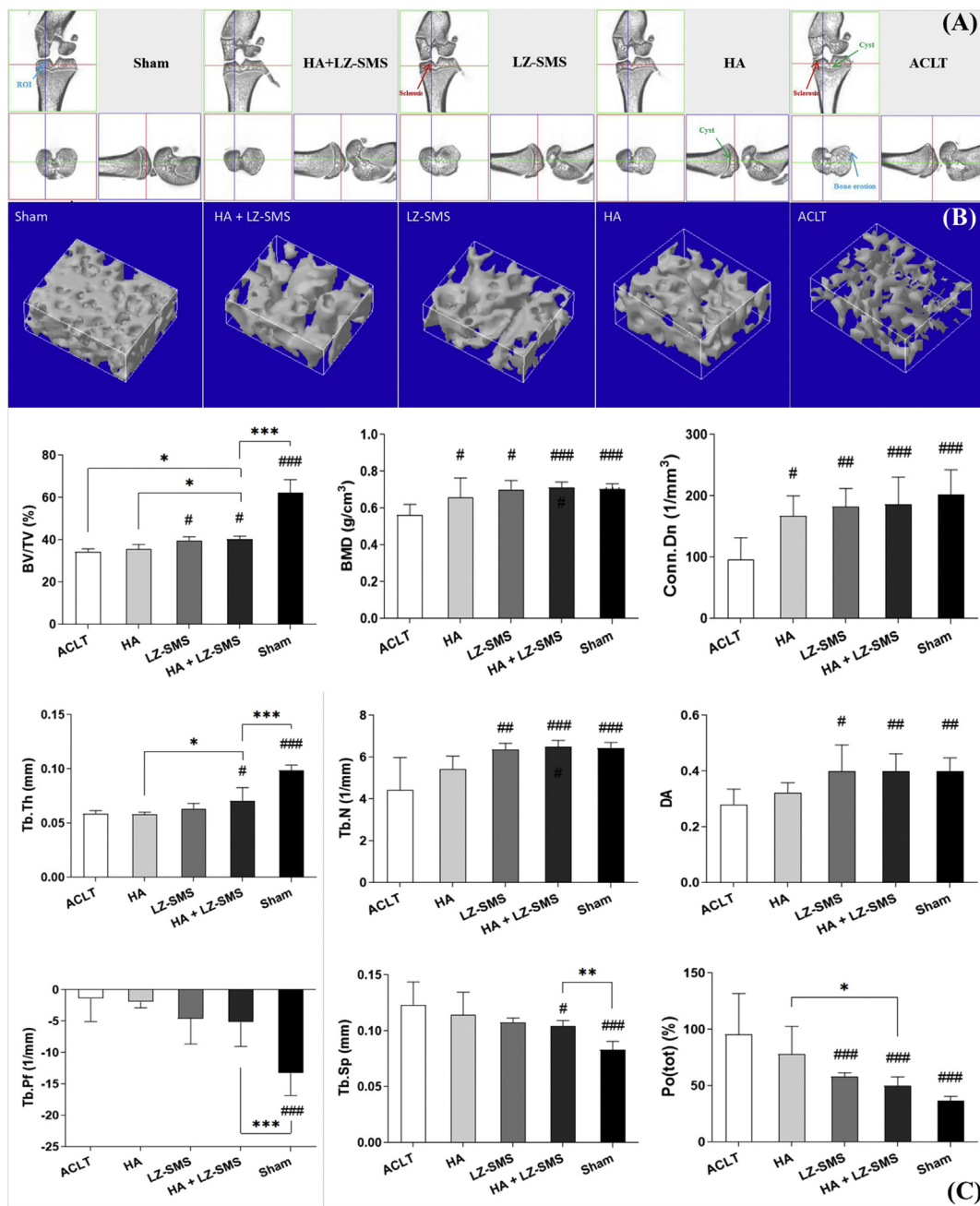
Figure 4. Micro-architecture of subchondral bone in the ACLT induced OA rats. (A) 3-view micro-CT images of the right hind knee joint of rats with different treatment. Blue arrow pointed blue rectangle is shown the region of interest (ROI) in Sham group. Blue arrow pointed bone erosion is shown in ACLT group. Red arrow pointed bone sclerosis at distal medial tibial SCB plate is shown in LZ-SMS and ACLT groups. Green arrow pointed SCB cysts are shown in ACLT and HA groups. (B) 3D micro-CT reconstruction images of the ROI under the loadbearing area of medial tibial SCB from rats with different treatment. (C) The Bar charts are shown with the mean values of detailed micro-architectural parameters of medial tibial SCB. Differences among each parameter are compared by one-way ANOVA (n = 5/group, #p < 0.05, ##p < 0.01, ###p < 0.0001, ACLT vs. other groups). Wilcoxon test is used to assess the differences between two different treatments (n = 5/group, *p < 0.05, **p < 0.01; ***p < 0.0001, HA+LZ-SMS vs. other groups). (For interpretation of the references to colour in this figure legend, the reader is referred to the Web version of this article.)

Protein–protein interaction analysis

The PPI analysis of the 64 overlapping targets of LZ-SMS and OA was shown in Fig. 5C. While no significant interactive proteins were not shown. The protein translation genes with large number of core edges are IL-6, CASP3, VEGFA, MYC, AR, EGFR, CCND1, REA, ESR1 and MAPK8. The network results suggest that the above-mentioned genes may represent the hub genes for OA development.

GO and KEGG enrichment analysis

The top 30 significant BPs (adjusted p < 0.05) determined by GO enrichment analysis are shown in Fig. 6A. Importantly, we found a lot of OA-related BPs including negative regulation of apoptotic process, aging, positive regulation of cell proliferation, response to cytokine, inflammatory response and positive regulation of angiogenesis. The pathway analysis was performed to explore the underlying mechanisms of LZ-SMS
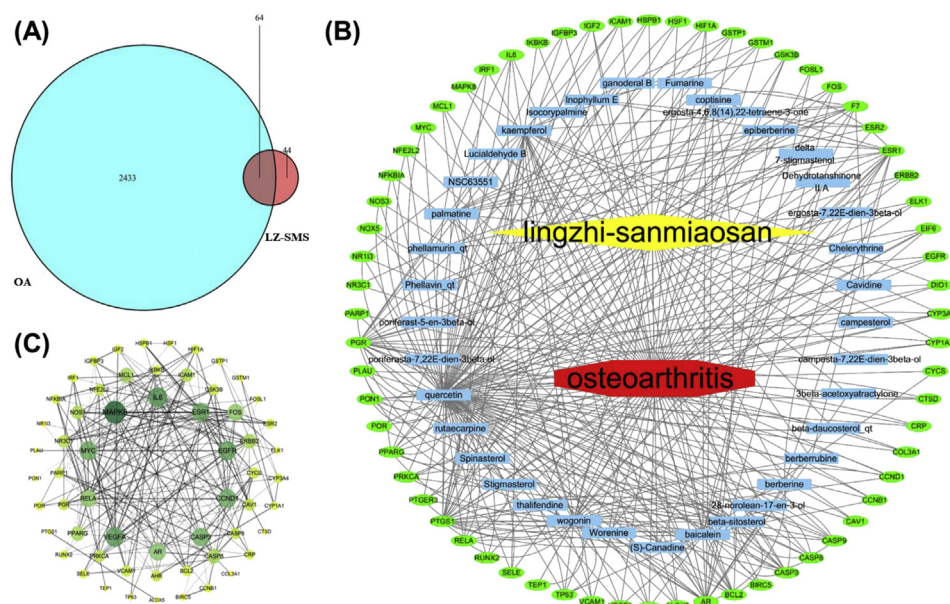
Figure 5. Active compound of LZ-SMS target-OA and protein–protein interaction (PPI) network analysis. (A) Venn diagram of drug-disease targets. The cyan circle represents 2496 known therapeutic targets for the treatment of OA. The red circle represents 108 known drug-targets of LZ-SMS. Totally 64 shared targets were shown between LZ-SMS and OA. (B) Active compound-target-disease network analysis. The blue rectangle represents active compound from LZ-SMS. The green oval represents the shared targets between LZ-SMS and OA. (C) The PPI analysis of 64 overlapping targets of LZ-SMS and OA. The nodes get larger with increasing degree. Edges: PPI between shared targets and their interactive partners. (For interpretation of the references to colour in this figure legend, the reader is referred to the Web version of this article.)
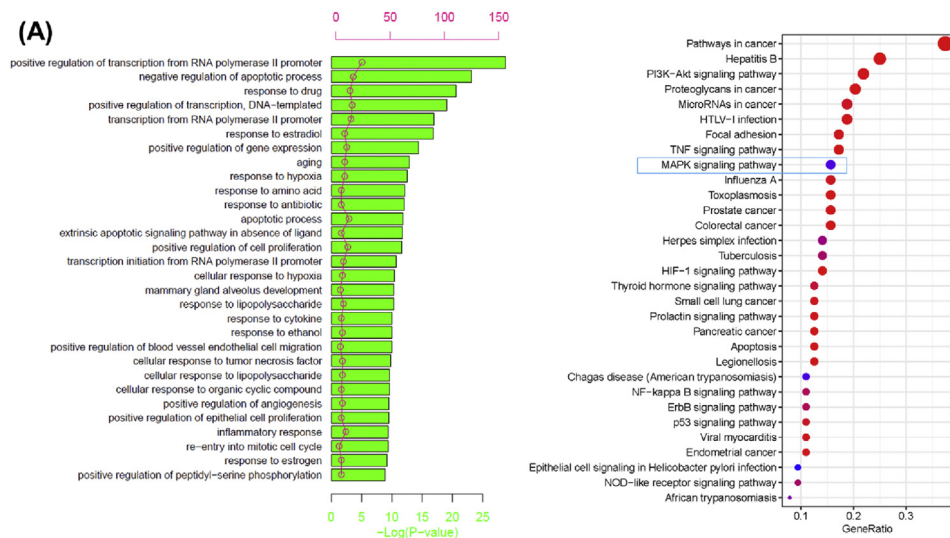

Figure 6. Gene Ontology (GO) enrichment and KEGG pathways analysis for 64 drug-disease targets. (A) The top 30 significant GO enrichment analysis. The red circle represents the gene count of each biological process. (B) The top 30 significant KEGG pathways. The blue rectangle shows the MAPK signaling pathway. The bigger of circles, the more targets are. The darker of color, the more significant is. (For interpretation of the references to colour in this figure legend, the reader is referred to the Web version of this article.)

action for treatment of OA. The 30 most significant pathways are shown in Fig. 6B (adjusted p < 0.05). PI3K/AKT signaling pathways, TNF signaling pathway and MAPK signaling pathway are considered to be the possible mechanism of treatment of OA.

Discussion

In the ACLT traumatic OA rat model, tibial trabecular bone undergoes osteoporosis to reply the changes of mechanical stresses environment [23]. In this study, we focused on the possible use of HA gel + LZ-SMS to improve current technologies for delivering drugs or therapeutic cells in promoting cartilage repair, and wished to incorporate injectable hydrogels and nanocarriers to enhance their delivery for clinical therapeutics [37–39]. Particularly, our results have confirmed that local injection of HA gel + LZ-SMS in the knee joint capsule implies an indirect preserve effect on maintaining the microstructural integrity of SCB that has strengthened and validated our previous conclusion: a stabilized physiological environment is essential to prevent AC degeneration [7]. The innovation of this study is the evaluation of a chondroprotective effect of

LZ-SMS on AC degeneration in the ACLT induced OA through enhancing the chondrogenic signals and cartilage matrix synthesis and microstructural integrity of tibial trabecular bone. Besides, we have shown the potential anti-inflammatory effect of HA gel + LZ-SMS and possible mechanism of LZ-SMS in elevating the chondrogenic signaling.

In the previous study, a decrease of proteoglycan contents and cartilage matrix was illustrated at the SZ of 6-month-old ACLT rats [29]. Moreover, the endochondral ossification at the CC layer indicated a pathological exacerbation of OA. Nevertheless, although the detection and analysis of AC were observed in a sole time point in this study, a less cartilage matrix and proteoglycan contents loss was observed, and no obvious fissures at cartilage area in HA+LZ-SMS group (Fig. 1A). Contrarily, the significantly higher volume ratios of HC/Sum and HC/CC represent a retrieval effect of LZ-SMS on AC in HA+LZ-SMS group (Fig. 1C and E). Therefore, we presume that the LZ-SMS may provide a direct protection on maintaining the cartilage matrix and proteoglycan contents of HC. Besides the obvious attenuated deterioration of the cartilage matrix and proteoglycan, we illustrated that there should be an indirect protective effect of LZ-SMS on tibial SCB, due

to the interaction between SCB and its upper layer AC, even in the relatively unstabilized load bearing status of traumatic OA model. In this study, with the HA gel + LZ-SMS treatment, the significantly elevated SCB parameters such as BV/TV, Tb.Th, BMD, Conn.Dn, Tb.N and DA, and the significantly decreased ones like Tb.Sp and Po(tot) revealed that maintaining the stabilization of SCB microstructure, in turn, could indirectly improve the physiological homeostasis in favor of suppressing the cartilage matrix degradation.

On the other hand, the synthesis of cartilage matrix could be induced by TGF-β via the Smad-dependent pathway in chondrogenic cell lines [40]. Otherwise, TGF-β can raise the number of chondrogenic cell to maintain the stabilization of AC [29,41]. In consistent with previous reports, in the present study, the chondrogenic signal levels of BMP2 and TGF-β1 at the MZ were significantly increased in HA gel + LZ-SMS treatment in ACLT traumatic OA (Fig. 2A–C). Even though, few studies have explored the mechanism of LZ-SMS in the chondrogenesis of AC and osteogenesis, we have found not only an upregulated chondrogenic signal *in vivo*, but also an elevated osteoblastic signal in the loadbearing area of tibial SCB that LZ-SMS can indirectly maintain the stabilization of AC by providing a basement of SCB microstructure (Fig. 4). Therefore, the HA gel + LZ-SMS treatment might have both supporting role in AC and SCB.

Clinically, improving the signals of articular chondrogenesis is a novel strategy for promoting cell recruitment into cartilage defects without injuring the SCB plate and for supporting the endogenous repair of degenerated cartilage as a compensatory approach for trauma-affected chondrocyte loss [41]. However, pro-inflammatory factors both IL-1β and TNF-α have profound influence on the local chondroprogenitor cell recruitment which could compromise the capability of endogenous cartilage repair or in situ regeneration of injured cartilage [41]. Fortunately, from the results of luminex multiplex assay, the production of TNF-α in synovial fluid was decreased in this study. Combined with the significantly decreased pro-inflammatory cytokines such as IFN-γ and IL-6 in plasma, as well as IL-12p70 and IL-6 in synovial fluid from the comparison between HA + LZ-SMS and ALCT groups (Fig. 3), this founding may imply a possible mechanism of LZ-SMS in suppressing pro-inflammatory factors and promoting chondrogenic cells differentiation to repair damaged cartilage. This offers a novel potential therapeutic option of LZ-SMS for cartilage retrieval via local administration in traumatic OA.

Furthermore, the MAPK signaling pathway has been found to play a distinct role on the synthesis and homeostasis of cartilage matrix, and the changes of these signaling molecules like p38 and ERK-1/2 perform a prominent role in chondrocyte dysfunction that is reported in the OA pathogenesis and progression [42,43]. During a normal chondrogenesis, suppression of MAPK signaling pathway resulted in a cartilage nodule formation [44]. Interestingly, our network analysis results of drug and OA presented 64 shared targets from 37 active compounds in LZ-SMS (Fig. 5A and B). In addition, according to the PPI analysis, the putative genes are including MAPK8 and IL-6, which represent core genes for the development of OA. These results indicated that besides the positive effect on chondrogenic signals, LZ-SMS could also interact with core proteins in OA development to regulate inflammatory circumstance, at least in part, through influencing the MAPK signaling pathway. Therefore, inhibiting the MAPK signaling pathway could impede OA onset and exacerbation. Meanwhile, almost no studies reported the cellular target of LZ-SMS in OA. Interestingly, our results demonstrated a downregulation of pro-inflammatory cytokines such as IL-17A, IL-12p70, TNF-α, INF-γ and IL-6 in HA gel + LZ-SMS treated OA rats (Fig. 3). Thus, from the results of evident downregulation of pro-inflammatory cytokines and putative core factors in MAPK signaling pathway, LZ-SMS may rescue the destruction of cartilage in ACLT induced OA. However, more detail mechanisms of LZ-SMS in how to affect the MAPK signaling pathways still needs to be further studied.

In conclusion, LZ-SMS can directly attenuate AC degeneration through activating the chondrogenic signaling pathway in a traumatic OA model. Meanwhile, the indirect effect on maintaining the integrity of SCB microstructure offers a stabilized physiological environment which is favorable to the cartilage recovery. Moreover, besides a synergistic anti-inflammatory effect, targeting the MAPK signaling pathway by local administration of HA gel + LZ-SMS may be a valid prevention strategy for weakening ACLT induced OA progression. We hope our studies could provide a clinical relevant approach using LZ-SMS to treat OA in future.

Conflict of Interest

The authors have no conflicts of interest to disclose in relation to this article.

Appendix A. Supplementary data

Supplementary data to this article can be found online at https://doi.org/10.1016/j.jot.2020.07.008.

References

[1] Kraus VB, Blanco FJ, Englund M, Karsdal MA, Lohmander LS. Call for standardized definitions of osteoarthritis and risk stratification for clinical trials and clinical use. Osteoarthritis Cartilage 2015;23(8):1233–41.

[2] Hayami T, Pickarski M, Zhuo Y, Wesolowski GA, RodanLe GA, Duong LT. Characterization of articular cartilage and subchondral bone changes in the rat anterior cruciate ligament transection and meniscectomized models of osteoarthritis. Bone 2006;38(2):234–43.

[3] Feng Y, Cai Z, Cheung WK, Yang KD, Xu L, Lu WW, et al. Multichromatic TTF staining characterizes cartilage matrix in osteoarthritisand bone development. Histol Histopathol 2019;34(3):275–86.

[4] Zhen G, Wen C, Jia X, Li Y, Crane JL, Mears SC, et al. Inhibition of TGF-beta signaling in mesenchymal stem cells of subchondral bone attenuates osteoarthritis. Nat Med 2013;19(6):704–12.

[5] Wang T, Wen CY, Yan CH, Lu WW, Chiu KY. Spatial and temporal changes of subchondral bone proceed to microscopic articular cartilage degeneration in Guinea pigs with spontaneous osteoarthritis. Osteoarthritis Cartilage 2013;21(4):574–81.

[6] Burr DB, Gallant MA. Bone remodelling in osteoarthritis. Nat Rev Rheumatol 2012; 8(11):665–73.

[7] Cai Z, Feng Y, Li C, Yang K, Sun T, Xu L, et al. Magnoflorine with hyaluronic acid gel promotes subchondral bone regeneration and attenuates cartilage degeneration in early osteoarthritis. Bone 2018;116(8):266–78.

[8] Muraoka T, Hagino H, Okano T, Enokida M, Teshima R. Role of subchondral bone in osteoarthritis development: a comparative study of two strains of Guinea pigs with and without spontaneously occurring osteoarthritis. Arthritis Rheum 2007; 56(10):3366–74.

[9] Gardner OFW, Musumeci G, Neumann AJ, Eglin D, Archer CW, Alini M, et al. Asymmetrical seeding of MSCs into fibrin-poly (ester-urethane) scaffolds and its effect on mechanically induced chondrogenesis. J Tissue Eng Regen Med 2017; 11(10):2912–21.

[10] Ding M, Odgaard A, Hvid I. Changes in the three-dimensional microstructure of human tibial cancellous bone in early osteoarthritis. J Bone Joint Surg Br 2003; 85(6):906–12.

[11] Day JS, Ding M, van der Linden JC, Hvid I, Sumner DR, Weinans H. A decreased subchondral trabecular bone tissue elastic modulus is associated with pre-arthritic cartilage damage. J Orthop Res 2001;19(5). 914-908.

[12] Setton LA, Zhu W, Mow VC. The biphasic porovisco-elastic behavior of articular cartilage: role of the surface zone in governing the compressive behavior. J Biomech 1993;26(4–5):581–92.

[13] Walsh DA, Bonnet CS, Turner EL, Wilson D, Situ M, McWilliams DF. Angiogenesis in the synovium and at the osteochondral junction in osteoarthritis. Osteoarthritis Cartilage 2007;15(7):743–51.

[14] Dougados M, Ayral X, Listrat V, Gueguen A, Bahuaud J, Beaufils P, et al. The SFA system for assessing articularcartilage lesions at arthroscopy of the knee. Arthroscopy 1994;10(1):69–77.

[15] Yu SL, Chan PK, Wong CK, Szeto CC, Ho S, So K, et al. Antagonist-mediated down-regulation of toll-like receptors increases the prevalence of human papillomavirus infection in systemic lupus erythematosus. Arthritis Res Ther 2012;14(2):R80.

[16] Szychlinska MA, Castrogiovanni P, Nsir H, Rosa MD, Guglielmino C, Parenti R, et al. Engineered cartilage regeneration from adipose tissue derived-mesenchymalstem cells: a morphomolecular study on osteoblast, chondrocyte andapoptosis evaluation. Exp Cell Res 2017;357(2):222–35.

[17] Krenn V, Morawietz L, Burmester GR, Kinne RW, Mueller-Ladner U, Muller B, et al. Synovitis score: discrimination between chronic low-grade and high-grade synovitis. Histopathology 2006;49(4):358–64.

[18] Schmitz N, Larerty S, Krans VB, Aigner T. Basic Methods in histopathology of joint tissues. Osteoarthritis Cartilage 2010;18(Suppl3):S113–6.

[19] Taruc-Uy RL, Lynch SA. Diagnosis and treatment of osteoarthritis. PrimaryCare 2013;40(4):821–36.

[20] Losina E, Weinstein AM, Reichmann WM, Burbine SA, Solomon DH, Daigle ME, et al. Lifetime risk and age at diagnosis of symptomatic knee osteoarthritis in the US. Arthritis Care Res (Hoboken) 2013;65(5):703–11.

[21] Kon E, Buda R, Filardo G, Martino AD, Timoncini A, Cenacchi A, et al. Platelet-rich plasma: intra-articular knee injections produced favorable results on degenerative cartilage lesions. Knee Surg Sports Traumatol Arthrosc 2010;18(4):472–9.

[22] Egemen A, Hayrettin K, Isik A. Intraarticular injections (corticosteroid, hyaluronic acid, platelet rich plasma) for the knee osteoarthritis. World J Orthoped 2014;5(3):351–61.

[23] Cui Z, Crane J, Xie H, Jin X, Zhen G, Li C, et al. Halofuginone attenuates osteoarthritis by inhibition of TGF-β activity and H-type vessel formation in subchondral bone. Ann Rheum Dis 2016;75(9):1714–21.

[24] Cai Z, Wong CK, Dong J, Jiao D, Chu M, Leung PC, et al. Anti-inflammatory activities of Ganoderma lucidum (Lingzhi) and San-Miao-San supplements in MRL/lpr mice for the treatment of systemic lupus erythematosus. Chin Med 2016;4(11):23.

[25] Chen DP, Wong CK, Leung PC, Fung KP, Lau CBS, Lau CP, et al. Anti-inflammatory activities of Chinese herbal medicine sinomenine and Liang Miao San on tumour necrosis factor-α-activated human fibroblast-like synoviocytes in rheumatoid arthritis. J Ethnopharmacol 2011;137(1):457–68.

[26] Bao YX, Wong CK, Li EK, Tam LS, Leung PC, Yin YB, et al. Immunomodulatory effects of Lingzhi and san-miao-san supplementation on patients with rheumatoid arthritis. Immunopharmacol Immunotoxicol 2006;28(2):197–200.

[27] Gui Y, Qiu X, Xu Y, Li D, Wang L. Bu-Shen-Ning-Xin decoction suppresses osteoclastogenesis via increasing dehydroepiandrosterone to prevent postmenopausal osteoporosis. Biosci Trends 2015;9(3):169–81.

[28] Yue R, Zhao L, Hu Y, Jiang P, Wang S, Xiang L, et al. Metabolomic study of collagen-induced arthritis in rats and the interventional effects of huang-lian-jie-du-tang, a traditional Chinese medicine. Evid Based Complement Alternat Med 2013;2013:439690.

[29] Cai Z, Hong M, Xu L, Yang K, Li C, Sun T, et al. Prevent action of magnoflorine with hyaluronic acid gel from cartilage degeneration in anterior cruciate ligament transection induced osteoarthritis. Biomed Pharmacother 2020;6(126):109733.

[30] Hahn H, Vogel M, Pompesius-Kempa M, Delling G. Trabecular bone pattern factorea new parameter for simple quantification of bone microarchitecture. Bone 1992;13(4):327–30.

[31] Ru J, Li P, Wang J, Zhou W, Li B, Huang C, et al. TCMSP: a database of systems pharmacology for drug discovery from herbal medicines. J Cheminf 2014;4(6):13.

[32] Stelzer G, Rosen N, Plaschkes I, Zimmerman S, Twik M, Fishilevich S, et al. The GeneCards suite: from gene data mining to disease genome sequence analyses. Curr Protoc Bioinform 2016;20(54). 1.30.1-1.30.33.

[33] OAa H, Scott AF, Amberger JS, Bocchini CA, McKusick VA. Online Mendelian Inheritance in Man (OMIM), a knowledge base of human genes and genetic disorders. Nucleic Acids Res 2005;1(33):D514–7.

[34] Lopes CT, Franz M, Kazi F, Donaldson SL, BOAer GD. Cytoscape Web: an interactive web-based network browser. Bioinformatics 2010;26(18):2347–8.

[35] Von MC, Martijn H, Daniel J, Steffen S, Peer B, Berend S. STRING: a database of predicted functional associations between proteins. Nucleic Acids Res 2003;31(1):258–61.

[36] Da WH, Sherman BT, Lempicki RA. Systematic and integrative analysis of large gene lists using DAVID bioinformatics resources. Nat Protoc 2009;4(1):44–57.

[37] Xu JB, Feng Q, Lin SE, Yuan WH, Li R, Li JM, et al. Injectable stem cell-laden supramolecular hydrogels enhance in situ osteochondral regeneration via the sustained co-delivery of hydrophilic and hydrophobic chondrogenic molecules. Biomaterials 2019;210(7):51–61.

[38] Kang HM, Zhang KY, Pan Q, Lin SE, Wong DSH, Li JM, et al. Remote control of intracellular calcium using upconversion nanotransducers regulates stem cell differentiation *in vivo*. Adv Funct Mater 2018:1802642.

[39] Zhu ML, Wei KC, Lin SE, Chen XY, Wu CC, Li G, et al. Bio-adhesive polymer some for localized and sustained drug delivery at pathological sites with harsh enzymatic and fluidic environment via supramolecular host-guest complexation. Small 2018;14(7):1702288.

[40] Van der Kraan PM, Blaney Davidson EN, Blom A, van den Berg WB. TGF-beta signaling in chondrocyte terminal differentiation and osteoarthritis: modulation and integration of signaling pathways through receptor-Smads. Osteoarthritis Cartilage 2009;17(12):1539–45.

[41] Joos H, Wildner A, Hogrefe C, Reichel H, Brenner RE. Interleukin-1 beta and tumor necrosis factor alpha inhibit migration activity of chondrogenic progenitor cells from non-fibrillated osteoarthritic cartilage. Arthritis Res Ther 2013;15(5):R119.

[42] Prasadam I, van Gennip S, Friis T, Shi W, Crawford R, Xiao Y. ERK-1/2 and p38 in the regulation of hypertrophic changes of normal articular cartilage chondrocytes induced by osteoarthritic subchondral osteoblasts. Arthritis Rheum 2010;62(5):1349–60.

[43] Prasadam I, Friis T, Shi W, van Gennip S, Crawford R, Xiao Y. Osteoarthritic cartilage chondrocytes alter subchondral bone osteoblast differentiation via MAPK signalling pathway involving ERK1/2. Bone 2010;46(1):226–35.

[44] Oh CD, Chang SH, Yoon YM, Lee SJ, Lee YS, Kang SS, et al. Opposing role of mitogen-activated protein kinase subtypes, erk-1/2 and p38, in the regulation of chondrogenesis of mesenchymes. J Biol Chem 2000;275(8):5613–9.